RADARSAT AND SNOW CHARACTERISTICS AT GREENLAND SUMMIT

Terhikki Manninen[(1)], Panu Lahtinen[(1)], Kati Anttila[(1,2)], Aku Riihelä[(1)]

[(1)]Finnish Meteorological Institute, P.O. Box 503, FI-00101 Helsinki, Finland, Email:terhikki.manninen@fmi.fi, panu.lahtinen@fmi.fi, kati.anttila@fmi.fi, aku.riihela@fmi.fi
[(2)]Finnish Geodetic Institute, Geodeetinrinne 2, FI-02430 Kirkkonummi, Finland, Email:kati.anttila@fmi.fi

ABSTRACT

The RASCALS (Radiation, Snow Characteristics and Albedo at Summit) campaign [1] was carried out at the Greenland Summit camp research station during June - July 2010. The collection of surface roughness, dielectric constant and density profiles of snow were carried out concurrently with snow albedo and bidirectional reflectance distribution function (BRDF) measurements. Polarimetric interferometry of Radarsat-2 quad pol fine beam images is used to study the snow surface anisotropy at Summit, Greenland. Various methods of determining the polarimetric coherence are tested and the results are compared with the in situ surface roughness results, which show a clear anisotropy varying with time. In addition, surface backscattering modelling is used to check the fraction of the surface backscattering.

1. INTRODUCTION

Surface roughness and grain size of snow have marked effects on the surface wind and surface albedo. Because the snow does not normally melt at all at the Greenland summit, the relatively small variation of the dry snow properties dominate the seasonal and diurnal variation of the snow surface. Surface roughness of varying magnitude determines the spatial variations in the wind velocity field [2]. Near the surface, the flow field is closely controlled by small-scale roughness elements that cause variations in wind speed and direction over short distances. Gradually, with increasing altitude, the dominant influence by micro roughness near the surface is transformed to control by large-scale terrain features higher in the air stream. The objective of this study is to find out what kind of information of the snow status it is possible to derive from polarimetric SAR images.

2. IN SITU MEASUREMENTS

2.1. RASCALS campaign

The RASCALS expedition spent over three weeks at the Summit camp research station (72°35'46.4"N, 38°25'19.1"W) near the top of the Greenland Ice Sheet during polar summer 2010 [1]. During this time, detailed measurements of the physical and optical properties of Arctic perennial snow were carried out concurrently with snow albedo and reflectance measurements. Favourable weather conditions during the campaign enabled the collection of a large dataset various snow properties. At the time of RASCALS campaign the Greenland summit was a place of snow accumulation without melting periods.

2.2. Snow measurements

The surface roughness data contains about 500 individual 1 m long profiles taken in 16 days. The rms height, correlation length and autocorrelation function (ACF) were determined as a function of length [3]. An example of the rms height and correlation length normalized with the wave number k are shown in *Fig. 1*. The surface roughness parameters values of a Radarsat SLC pixel (4.7 m) are within the validity range of the small scale perturbation (SPM) backscattering model [4]. All of the profiles better the multiscale ACF types matched than the single scale ones [3]. About half of the cases (227) were of the multiscale exponential type:

$$\rho(\xi) = (1+2b)\left(\frac{|\xi|}{k_0 x_0}\right)^{1+2b} \Gamma\left(-1-2b, \frac{|\xi|}{k_0 x_0}\right) \qquad (1)$$

Here b is a multiscale roughness parameter, which for a fBm surface equals the Hurst coefficient [3] and equals 2-D, D being the fractal dimension. The correlation length and the rms height at distance x_0 are $L = k_0 x_0$ and $\sigma = c\, x_0^{\,b}$, where c is a constant. The variation of the parameter b with the azimuth angle is shown in *Fig. 2*.

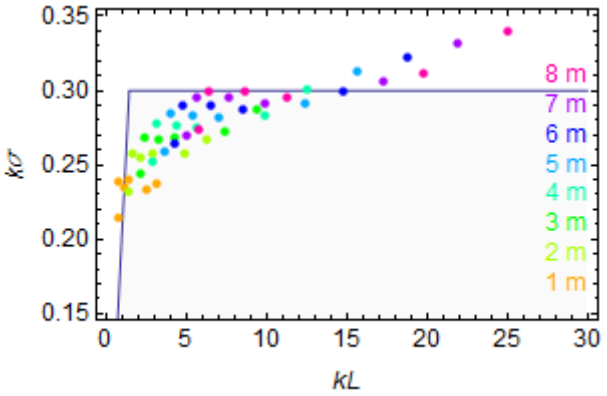

Figure 1. Measured normalized rms height as a function of the normalized correlation length in July 10, 2010. The marker colour indicates the length for which the values are determined. The validity range of the SPM backscattering model is shaded.

Proc. 'ESA Living Planet Symposium 2013', Edinburgh, UK
9–13 September 2013 (ESA SP-722, December 2013)

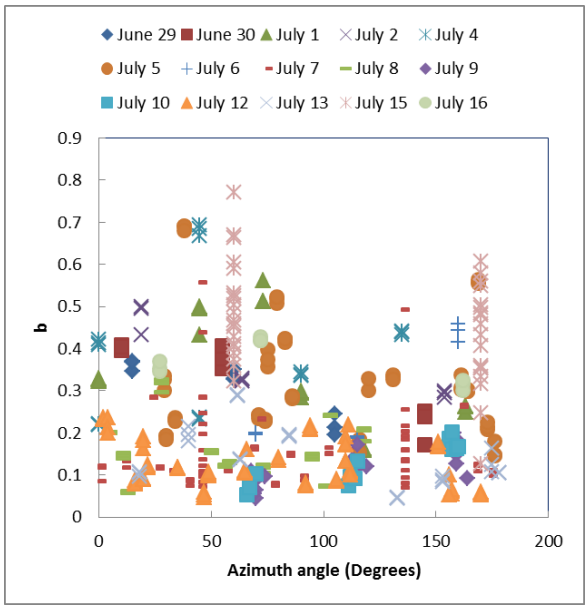

Figure 2. Measured variation of the distance dependence related parameter b of the rms height ($\sigma = c\, x_0^{b}$) as a function of the azimuth direction of the surface roughness profile.

Although the variation within the day can be large, it seems that the azimuth directions of about 60° (240°) and 180° (360°) tend to have higher roughness parameter *b* values. The same variation is evident also in the rms height and correlation length data.

The dielectric constant and density of snow were obtained in 8 days for profiles of about 1 m deep with an interval of about 5 cm. In addition, the density was analysed down to 2 m in one snow pit. The Toikka snow fork [5] was used for the permittivity measurements. The snow densities were sampled using Snowmetrics RIP Cutter 2 [6]. The obtained 250 cm^3 samples were emptied to a small plastic bag and weighted, tared and converted to density values. The results are shown in *Figs. 3 – 5*. The slight variation in the dielectric constant is attributed to the measurement inaccuracy.

2.3. Weather data

The Greenland Summit has a continuously operating weather station and the hourly values for air temperature [*Fig. 6*], wind speed and direction, relative humidity, atmospheric pressure, snow temperature and surface albedo were available for the whole year 2010 [9].

3. SAR IMAGES

Radarsat-2 SLC Fine Quad Polarization SAR data were available for a period from May to August, 2010. Two incidence angles were chosen for the study: 33.3° (FQ13) and 47.5° (FQ29). Large incidence angles were preferred as the study concentrated on surface

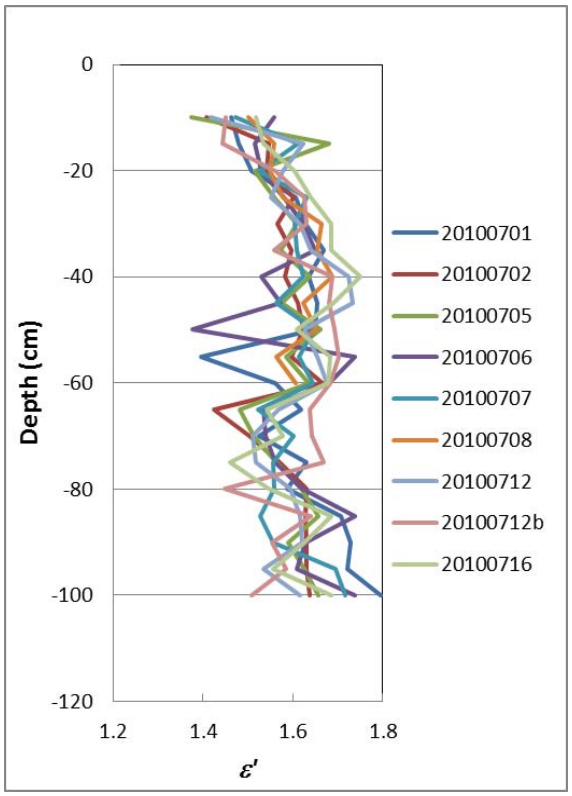

Figure 3. Measured real part of the snow dielectric constant during the RASCALS campaign.

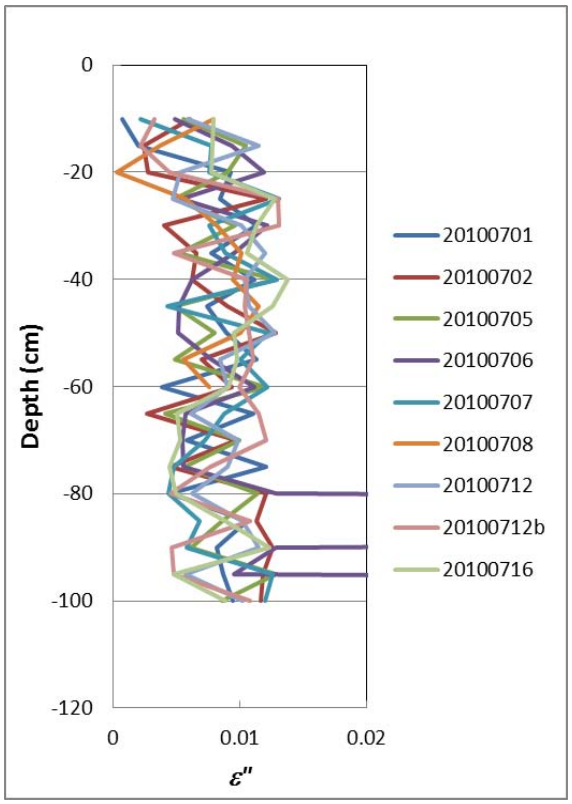

Figure 4. Measured imaginary part of the snow dielectric constant during the RASCALS campaign.

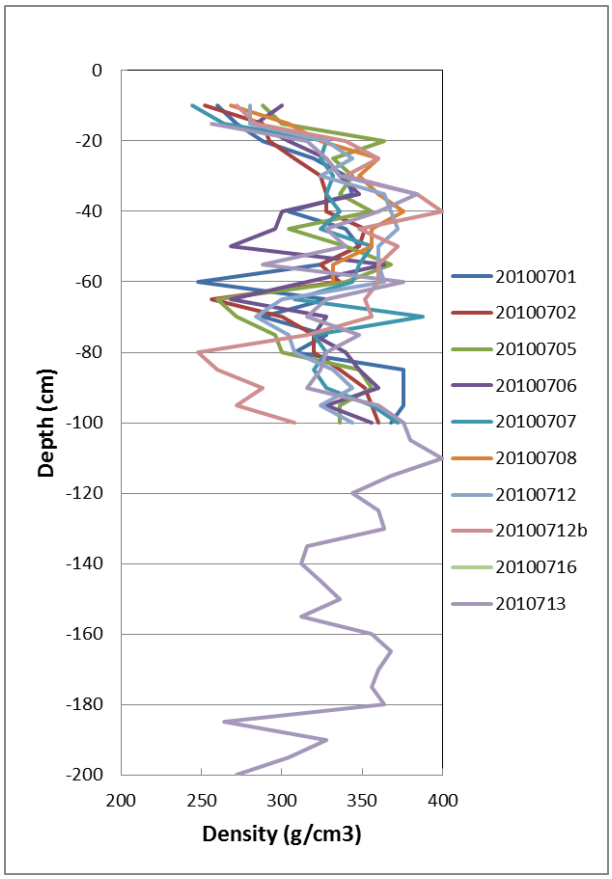

Figure 5. Measured snow density during the RASCALS campaign.

roughness detection. Ten images of each beam were ordered, but unfortunately one image during the campaign was cancelled. The intersection of all SAR images was used as a basis for the study for which all average parameter values were determined.

4. METHODS

The surface backscattering coefficient was determined for the days of surface roughness measurements as a function of length included in the calculations using the SPM model [4]. Both the single scale and multi scale exponential autocorrelation functions were used in the calculations. The volume backscattering was then estimated by subtracting the surface backscattering from the total backscattering obtained from the SAR images. The grain size was estimated from the snow volume backscattering σ_v^0 using the following formulas (2) … (6) [7]

$$\sigma_v^0 = \frac{1}{2}\frac{\cos\theta}{\frac{1}{\varsigma^3|K|^2}\mathrm{Im}\{-K\}+\frac{2}{3}} \quad (2)$$

where [4]

$$\mathrm{Im}\{-K\} \approx \frac{3\varepsilon''}{(\varepsilon'+2)^2} \quad (3)$$

Table 1. Radarsat-2 images available for the study.

Date	Time [UTC]	Orbit	Incidence angle [Degrees]
May 7, 2010	08	DES	47.5
May 11, 2010	20	ASC	47.5
May 19, 2010	19	ASC	33.3
May 23, 2010	09	DES	33.3
May 31, 2010	08	DES	47.5
June 4, 2010	20	ASC	47.5
June 12, 2010	19	ASC	33.3
June 16, 2010	09	DES	33.3
June 24, 2010	08	DES	47.5
June 28, 2010	20	ASC	47.5
July 10, 2010	09	DES	33.3
July 18, 2010	08	DES	47.5
July 22, 2010	20	ASC	47.5
July 30, 2010	19	ASC	33.3
August 3, 2010	09	DES	33.3
August 11, 2010	08	DES	47.5
August 15, 2010	20	ASC	47.5
August 23, 2010	19	ASC	33.3
August 27, 2010	09	DES	33.3

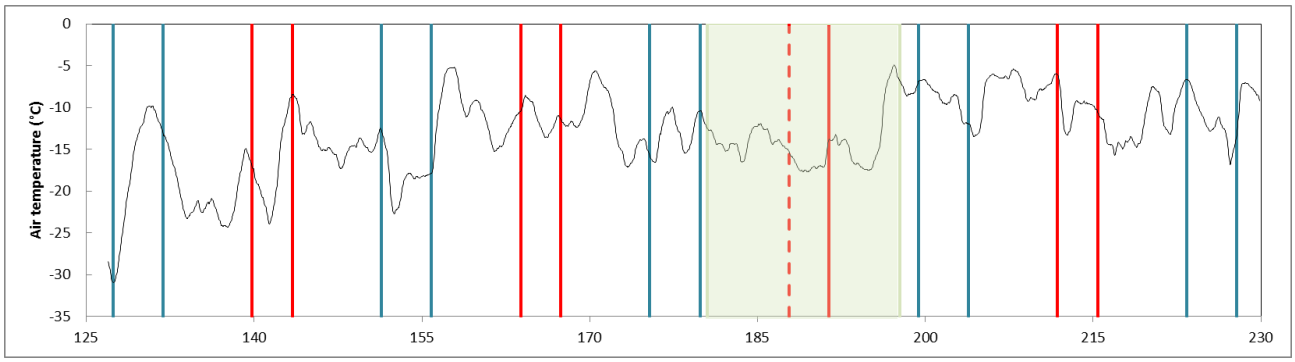

*Figure 6. Radarsat-2 images available (**FQ13** and **FQ29**), the RASCALS campaign measurement period (olive shade) and the variation of moving average air temperature within 24 hours at the Greenland summit station. The dashed line indicates the timing of the Radarsat-2 image ordered but cancelled.*

and electric size of the particle is $\varsigma = \frac{2\pi r}{\lambda}$,

where r is the actual size of the particle, λ is the wavelength used, θ is the incidence angle of the incoming radiation and ε' and ε" are the real and imaginary parts of the dielectric constant of snow.

Further on,

$$|K|^2 = \left|\frac{\dot{m}^2 - 1}{\dot{m}^2 + 2}\right|^2 \quad (4)$$

where $m = n + j\eta$ is the refractive index of snow and n and η are the real and imaginary parts of the refractive index, respectively. They are obtained from the dielectric constant [7]

$$n = \left[0.5 \cdot \left(\sqrt{(\varepsilon')^2 + (\varepsilon'')^2} + \varepsilon'\right)\right]^{0.5} \quad (5)$$

$$\eta = \left[0.5 \cdot \left(\sqrt{(\varepsilon')^2 + (\varepsilon'')^2} - \varepsilon'\right)\right]^{0.5} \quad (6)$$

The penetration depth δ_p was estimated from [8]

$$\delta_p = \frac{\lambda}{4\pi}\left\{\left[\left(1 + \left(\frac{\varepsilon''}{\varepsilon'}\right)^2\right)^{1/2} - 1\right]\frac{\varepsilon'}{2}\right\}^{-1/2} \quad (7)$$

As the dielectric constant and density of snow did not show variation from day to day during the RASCALS campaign within the accuracy of the measurements, constant (average) values ε'=1.631, ε"=0.0066 and ρ = 338.3 g/cm^3, respectively, were used for them in the calculations. Moreover, it was known that snow did not melt in summer 2010 at the Greenland summit. Hence, it was assumed that the volume scattering was constant during the summer. Then the surface scattering can be taken to be linearly dependent on the total backscattering available in the SAR images.

The effect of snow surface roughness on the SAR signal was studied both using the actual backscattering coefficients and the following three polarimetric coherence coefficients reported to be sensitive to surface roughness [12, 13, 14, 15]

$$\gamma_{HHVV} = \frac{\left|< S_{HH} S_{VV}^* >\right|}{\sqrt{< S_{HH} S_{HH}^* >< S_{VV} S_{VV}^* >}} \quad (8)$$

$$\gamma_{(HH+VV)(HH-VV)} = \frac{\left|< (S_{HH} + S_{VV})(S_{HH} - S_{VV})^* >\right|}{\sqrt{< |S_{HH} + S_{VV}|^2 >< |S_{HH} - S_{VV}|^2 >}} \quad (9)$$

$$\gamma_{LLRR} = \frac{\left|< S_{LL} S_{RR}^* >\right|}{\sqrt{< S_{LL} S_{LL}^* >< S_{RR} S_{RR}^* >}} \quad (10)$$

Here S refers to the complex scattering amplitude of the object and * indicates the complex conjugate. Also the usefulness of the magnitude of the real part of γ_{LLRR} was checked [16].

For the azimuthal anisotropy analysis, the polarimetric coherence was calculated so that S_{HH} and S_{VV} were taken from different parts of the image in a 3x3 window. 10000 randomly located window pairs were selected and the coherence was averaged in each azimuth direction with one degree interval using the number of pairs of each distance between window centres as the weight in averaging.

5. RESULTS

The level of the surface backscattering is roughly the same when using single or multi scale autocorrelation function, but for larger distances included in the backscattering coefficient value the multiscale version produces slightly higher values, as is natural. [*Figs. 7* and *8*].

The volume scattering dominated the surface scattering as expected, since the dielectric constant is small and the snow layer is semi-infinite. The fraction of volume scattering in July 10, 2010 exceeded 90% for all cases and lengths studied [*Figs. 7 and 8, Table 2*]. In addition, the fraction of volume scattering was practically identical for both polarizations, the mean value being 0.9997 for the volume scattering ratio for VV/HH.

The grain size values for July 10, 2010 were calculated using Eqs. 2 - 6, [*Fig. 9*]. They varied slightly depending on the polarization, but the use of single or multi scale ACF did not play a role. In the calculations it was assumed that the snow pack is isotropic. Understandably, there will be some horizontal structuring in the upper most 1.7 m thick layer (corresponding to the penetration depth in C-band according to Eq. 7), due to weather conditions during the accumulation. Accordingly, this will show up in the difference of the vertical and horizontal estimates of the grain size. The calculated grain size values are about the

Table 2. Fractions of calculated volume backscattering for July 10, 2010.

Polarization	Scale	Min(σ_v^0/σ^0) [%]	Max(σ_v^0/σ^0) [%]
HH	Single	92.0	99.5
HH	Multi	92.8	98.8
VV	Single	91.9	99.5
VV	Multi	92.8	98.8

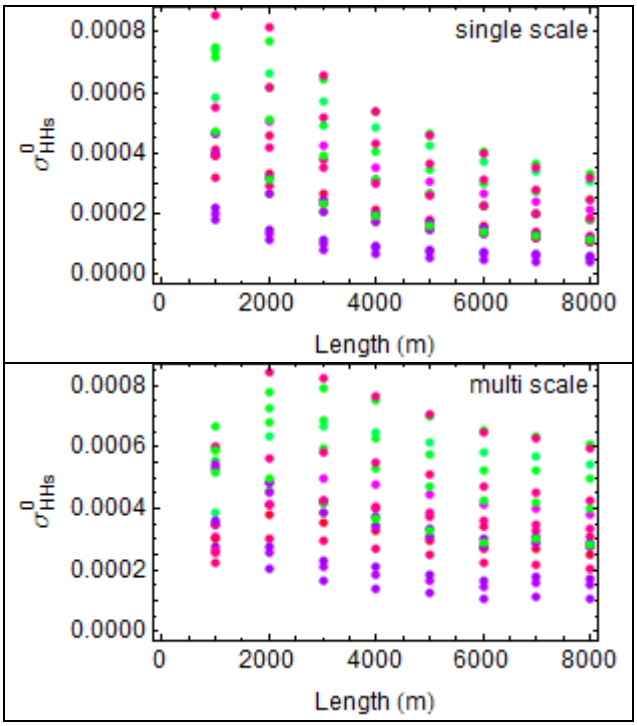

*Figure 7. The horizontal polarization surface backscattering coefficients for July 10, 2010 calculated using single scale and multi scale exponential autocorrelation functions. The colours correspond to three azimuth directions of the surface roughness measurements (**68°-70°**, **113°-119°**, **158°-164°**).*

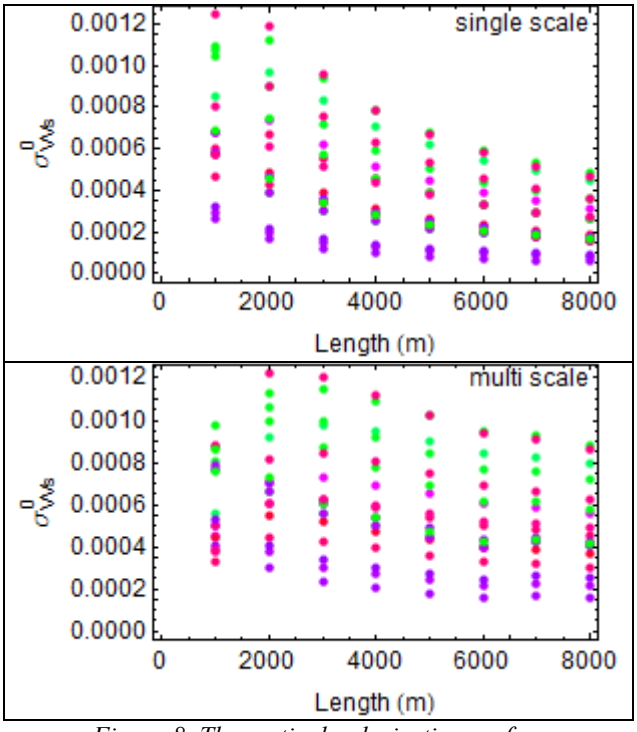

Figure 8. The vertical polarization surface backscattering coefficients for July 10, 2010 calculated using single scale and multi scale exponential autocorrelation functions. The colours are as in Fig.7.

same as the measured grain size values at about half a meter's depth [*Fig. 10*]. In July 10 only surface grains were measured, therefore grain size measurements of July 12 were used for comparison.

The specific surface area (SSA) values corresponding to the estimated grain radii of *Fig. 9* vary in the range of 2.4 … 2.5 m^2/kg. The SSA values determined from optical measurements in July 10 are of the order of 10 … 30 m^2/kg, depending on the model and shape of the grain used. As the penetration depth in microwaves is markedly larger than in the optical wavelength range and the grains tend to be larger and less concave in the lower parts of the snow pack, the estimated microwave and optical based SSA values are in line.

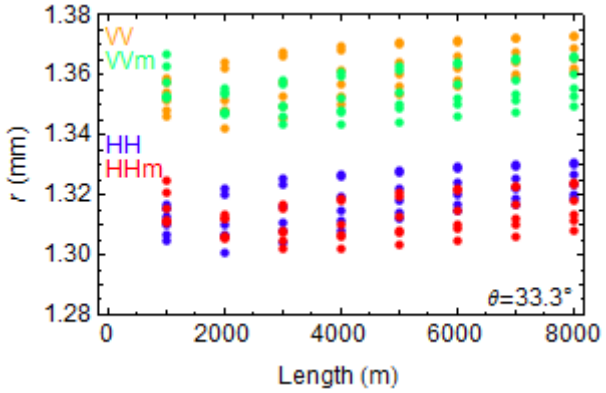

Figure 9. The radii of the snow grains calculated from the backscattering coefficients, surface roughness and permittivity measurements. Both single scale and multi scale (m) autocorrelation functions were used for HH and VV polarizations.

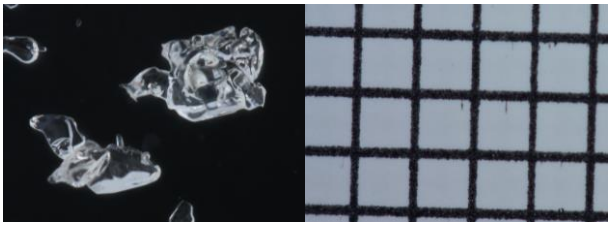

Figure 10. An example of the snow grains measured at the depth of 36 … 50 cm in July 12, 2010. The grid spacing is 1 mm.

The temporal variation of the total backscattering in the Radarsat-2 data shows a systematic trend during the summer for both polarizations and beams [*Fig. 11*]. In addition, the morning backscattering coefficient values were markedly higher than those observed in the evening for the smaller incidence angle and slightly higher for the larger incidence angle case. A second order polynomial fitted well in each separate case (beam, polarization, time of day) and the coefficients of determination for the regressions varied in the range R^2 = 0.83 … 0.996, the evening values being in every case higher than 0.97.

For γ_{HHVV} *and* $\gamma_{(VV+HH)(VV-HH)}$ both the seasonal variation and the difference between morning and evening data was less systematic for both beams [*Fig. 12*]. Moreover, the behaviour of the coherence coefficients was not similar for the two incidence angles. An interesting incidence angle dependence was observed for γ_{LLRR} and its real part's magnitude [*Fig. 13*]. For the larger incidence angle the seasonal evolution of its evening value had an increasing trend until July (R^2 = 0.84 … 0.999), whereas for the smaller incidence angle the opposite behaviour was observed. For the morning values the shape of the seasonal variation was essentially similar for both beams. For the larger incidence angle the difference between morning and evening values of γ_{LLRR} was markedly larger than for the smaller incidence angle.

The circular polarization correlation coefficient γ_{LLRR} is in a wide range independent on the dielectric constant and depends only on the surface roughness [15]. The smaller incidence angle γ_{LLRR} values suggest an increasing trend for the surface roughness in early summer, but the larger incidence angle data points to the opposite direction. The larger incidence angle backscattering should be more sensitive to surface roughness than the small incidence angle backscattering, and indeed the difference between the morning and evening values of γ_{LLRR} is larger for beam FQ29. As the surface contributes only a little to the total backscattering, it is understandable, that the backscattering coefficient of beam FQ29 changes only slightly. It is striking, how large the difference between the morning and evening backscattering coefficient values are for beam FQ13. Possibly this is due to the steeper incidence angle being better able to detect

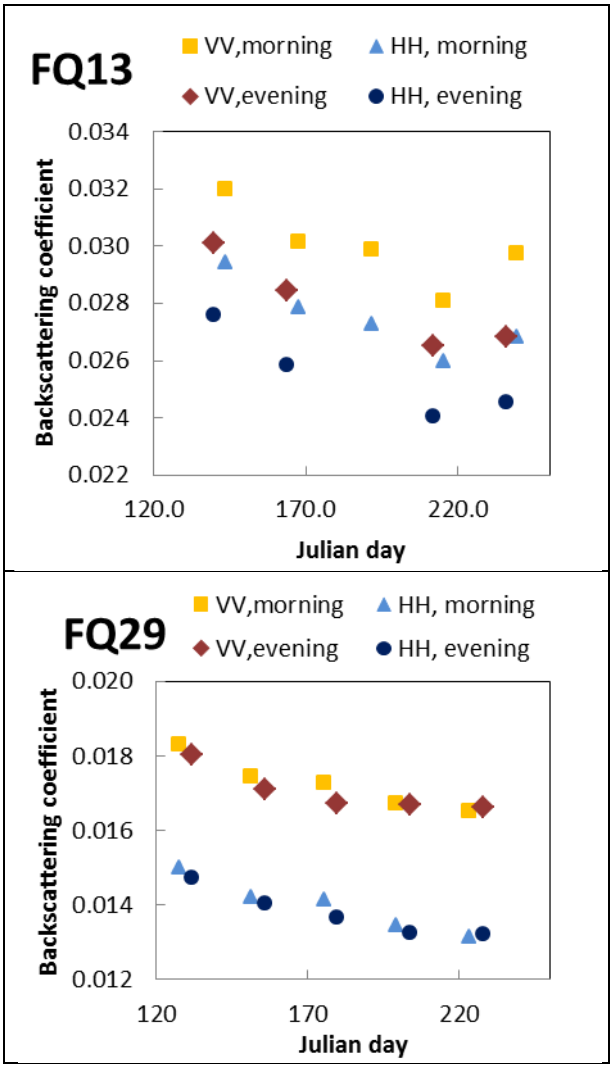

Figure 11. Variation of the VV and HH backscattering coefficient of beams FQ13and FQ29 with time for morning and evening images.

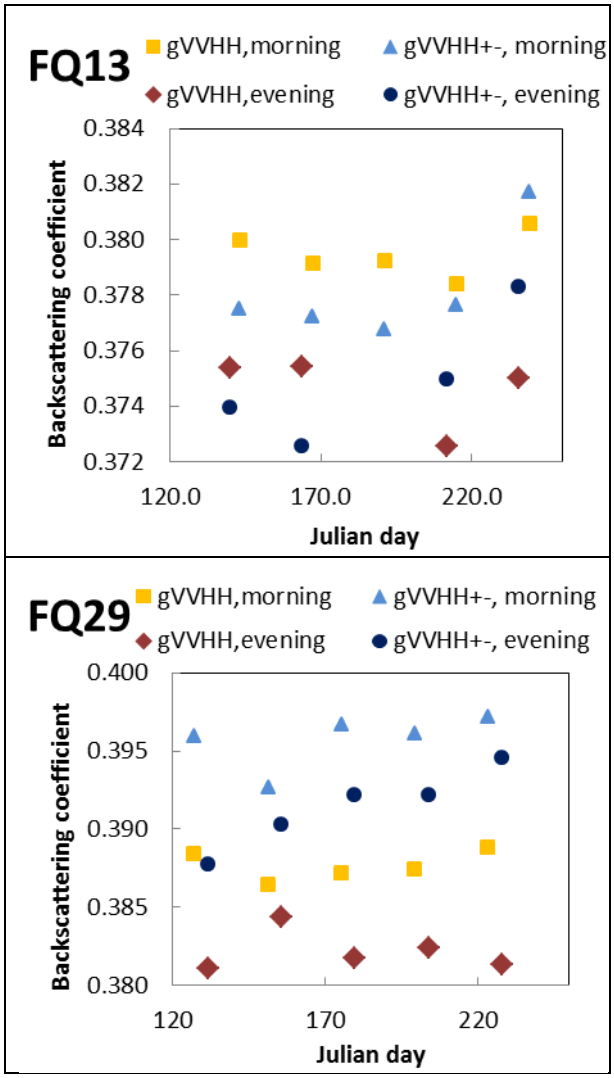

Figure 12. Variation of the coherence coefficient γ_{HHVV} *and* $\gamma_{(VV+HH)(VV-HH)}$ *of beams FQ13and FQ29 with time for morning and evening images.*

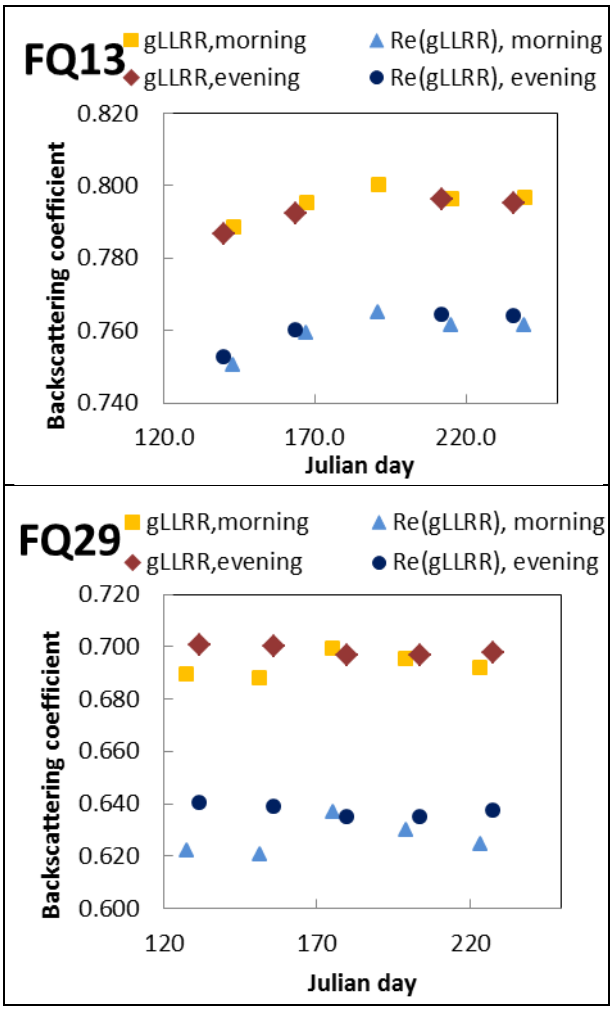

Figure 13. Variation of the coherence coefficient γ_{LLRR} and the absolute value of its real part of beams FQ13 and FQ29 with time for morning and evening images.

the 3D structure and pits of the surface hoar layer. It seems that the surface hoar layer is thick enough to constitute a separate volume scattering layer having a large amount of air in it. The effective permittivity of this fluffy layer is very small and causes a difference in the volume scattering component. The larger incidence angle does not detect the vertical air pockets as clearly.

The difference in the VV total (and calculated surface) backscattering coefficient caused by the surface hoar was 5.9% … 11% (6.2% … 11%) for the beam FQ13, but only 1.5 … 3% (0.5 … 3.2%) for the beam FQ29. For HH polarization the corresponding variation ranges were 6.6% … 9.2% (6.6% … 9.2%) and 1.1% … 3.4 % (0.4 …3.4%). In estimating the surface backscattering part, it was assumed that the difference between the total backscattering and surface backscattering was the same as for July 10, for which the surface backscattering could be modelled on the basis of the surface roughness data available. The surface hoar effect on γ_{LLRR} was in all cases smaller than 2%.

Despite of the small permittivity of snow and the small fraction of surface backscattering, Radarsat-2 images can be used also for surface hoar detection, not only hoar in the inner parts of the firn [11]. At the Greenland summit, the importance of hoar frost is mainly in its effect on albedo and on the friction wind via surface roughness [10]. In mountainous areas depth hoar is reported to play an essential role in avalanche release [10]. Thus the capability of SAR to detect hoar formation is valuable for avalanche forecasting.

The anisotropy of the ice fields was studied using internal coherence within two points of the image [*Fig. 14*]. It turned out that there is a reasonable positive correlation (R^2 = 0.7) with the normalized correlation length *kL* and the polarimetric coherence $\gamma_{(VV+HH)(VV-HH)ij}$, where *ij* indicates that one polarization is calculated in a window located at pixel i and the other one in a window located at pixel j. Simultaneous surface roughness data and SAR images were available only on July 10, but June 28 vs. 29 and July 16 vs. 18 were considered close enough matches to be included in the analysis.

Some of the scatter in *Fig. 14* is caused by the fact, that every pixel of the SAR image is measured in the same direction, whereas the surface roughness profiles were measured in (essentially) three directions on each day. The reason that it is sometimes still possible to detect the dominant roughness direction of the target area is based on strong enough anisotropy in the surface height statistics, which will then affect the phase difference statistics of pixel pairs. If more data were available this matter would be studied more thoroughly, as it would be really valuable, if the anisotropy of the surface roughness of the snow field could be detected with SAR data, because the roughness affects the wind field at the surface.

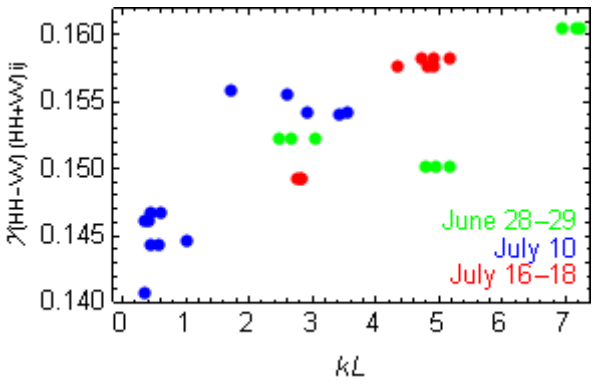

Figure 14. Relationship between the normalized correlation length measured in June 29, July 10 and July 16, and the polarimetric coherence $\gamma_{(VV+HH)(VV-HH)ij}$ calculated from images of June 28, July 10 and July 18.

6. CONCLUSIONS

Radarsat-2 VV and HH backscattering coefficients provide reasonable grain size information of the snow pack at the Greenland summit. The seasonal surface roughness evolution is also manifested in the backscattering coefficient values. The hoar formation can be detected both using the backscattering coefficients and various polarimetric coherence parameters. The circular polarization correlation coefficient used in combination with the backscattering coefficients help in concluding, whether the observed change is caused by alteration in surface or volume backscattering or both. Preliminary results indicate that it may be possible to study the anisotropy of the target surface roughness by using polarimetric interferometric coherence within image.

7. ACKNOWLEDGEMENTS

Radarsat data were provided by ESA via the EU SOAR project, ID 6759 (ARCS). This work was financially supported by the Emil Aaltonen Foundation and the EUMETSAT visiting scientist program of the CM-SAF project.

8. REFERENCES

[1] A. Riihelä, P. Lahtinen, T. Hakala, "The radiation, snow characteristics and albedo at summit (RASCALS) expedition report", Finnish Meteorological Institute Report 2011:8, 46 p., 2011.

[2]H. Granberg, "Indirect mapping of the snowcover for permafrost prediction at Schefferville, Quebec" in Proceedings of the North American Contribution Permafrost, Second Internaitonal Conference, 13-28 July 1973, 113-120.

[3] A.T. Manninen, 2003, "Multiscale surface roughness description for scattering modelling of bare soil", Physica A 319, 535-551.

[4] Ulaby, F.T., Moore, R.K. and Fung, A.K., 1982, Microwave remote sensing: Active and passive, Vol. II: Radar remote sensing and surface scattering and emission theory, Addison-Wesley, Reading, MA.

[5] A. Sihvola and M. Tiuri, 1986, "Snow fork for field determination of the density and wetness profiles of a snow pack", IEEE Trans. Geosci. Remote Sens., 24(5):717–721

[6] http://www.snowmetrics.com/store/rip-2-cutter-250-cc-p-181.html.

[7] Boris Yurchak, 2009, "Some Features of The Volume Component of Radar Backscatter From Thick and Dry Snow Cover", Advances in Geoscience and Remote sensing, Gary Jedlovec (Ed.), ISBN: 978-953-307-005-6.

[8]Barber, D. G. & LeDrcw. E. F., 1994, Modeling synthetic aperture radar (SAR) scattering from a seasonally varying snow-covered sea icc volume at 5.3 and *9.25* GHz. *Polar Research 13.* 35-54.

[9] Steffen, K., J. E. Box, and W. Abdalati, 1996, Greenland Climate Network: GC-Net, in Colbeck, S. C. Ed. CRREL 96-27 Special Report on Glaciers, Ice Sheets and Volcanoes, trib. to M. Meier, pp. 98-103.

[10] Hachikubo, A. and Akitaya, E., 1997, "Effect of wind on surface hoar growth on snow", J. Geophys. Res., *102*, D4, 4367-4373.

[11] Ng, F. and King, E.C., 2013, "Formation of RADARSAT backscatter feature and undulating firn stratigraphy at an ice-stream margin ", Annals of Glaciology 54(64) 2013 doi:10.3189/2013AoG64A202.

[12] Borgeaud, M. and Noll, J., 1994, "Analysis of Theoretical Surface Scattering Models for Polarimetric Microwave Remote Sensing of Bare Soils", International Journal of Remote Sensing, *15*(14), 2931-2942.

[13] S.R. Cloude and K.P. Papathanassiou, "Polarimetric SAR Interferometry", IEEE Transactions on Geoscience and Remote Sensing", Vol. 36, No. 5, pp.1551-1564, 1998.

[14] Hajnsek, I., 2001, "Inversion of Surface Parameters Using Polarimetric SAR", DLR-Science Report, *30*, ISSN 1434-8454, 224 p.

[15] Mattia, F., T. Le Toan, J.C. Souyris, G. De Carolis, N. Floury, F. Posa and G. Pasquariello, , 1997 , "The effect of surface roughness on multi- frequenzy polarimetric SAR data". IEEE Trans. Geosci. Remote Sensing, *35,* 954-966.

[16] Schuler, D. L., J.S. Lee and D. Kasilingam, 2002,"Surface roughness and slope measurements using polarimetric SAR data". IEEE Trans. Geosci. Remote Sensing, *40*, 687-698.